

1 **NgAgo-enhanced homologous recombination in *E. coli* is mediated by DNA**  
2 **endonuclease activity**

3 Kok Zhi Lee<sup>1</sup>, Michael A. Mechikoff<sup>1</sup>, Archana Kikla<sup>2</sup>, Arren Liu<sup>2</sup>, Paula Pandolfi<sup>2</sup>, Frederick S. Gimble<sup>3,4</sup>,  
4 and Kevin V. Solomon<sup>1,2\*</sup>

5 <sup>1</sup>Department of Agricultural and Biological Engineering, Purdue University, West Lafayette, IN 47906,  
6 USA.

7 <sup>2</sup>Department of Biological Sciences, Purdue University, West Lafayette, IN 47906, USA.

8 <sup>3</sup>Purdue University Interdisciplinary Life Science Program (PULSe), Purdue University, West Lafayette,  
9 IN, 47906, USA.

10 <sup>4</sup>Department of Biochemistry, Purdue University, West Lafayette, IN, 47906, USA.

11

12 \* To whom correspondence should be addressed. Tel: +1 765-494-1134; Fax: +1 765-496-1115; Email:  
13 [kvs@purdue.edu](mailto:kvs@purdue.edu)

14

15 **ABSTRACT**

16 Prokaryotic Argonautes (pAgos) have been proposed as more flexible tools for gene-editing as they do not  
17 require sequence motifs adjacent to their targets for function, unlike popular CRISPR/Cas systems. One  
18 promising pAgo candidate, from the halophilic archaeon *Natronobacterium gregoryi* (NgAgo), however, has  
19 been subject to intense debate regarding its potential in eukaryotic systems. Here, we revisit this enzyme  
20 and characterize its function in prokaryotes. NgAgo expresses poorly in non-halophilic hosts with the  
21 majority of protein being insoluble and inactive even after refolding. However, we report that the soluble  
22 fraction does indeed act as a DNA endonuclease. Structural homology modelling revealed that NgAgo  
23 shares canonical domains with other catalytically active pAgos but also contains a previously unrecognized  
24 single stranded DNA binding domain (repA). Both repA and the canonical PIWI domain participate in DNA  
25 cleavage activities. We also found that these endonuclease activities are essential for enhanced NgAgo-  
26 guided homologous recombination, or gene-editing, in *E. coli*. Collectively, our results provide insight into  
27 the poorly characterized NgAgo for subsequent gene-editing tool development and sheds new light on  
28 seemingly contradictory reports.

29

## 30 INTRODUCTION

31 Long prokaryotic Argonaute proteins (pAgos) are programmable endonucleases that have recently been  
32 proposed as flexible tools for genome editing<sup>1</sup>. Like Cas9-based gene editing strategies, single-stranded  
33 nucleic acids bind to pAgos and enhance pAgo cleavage of complementary target nucleic sequences,  
34 enabling DNA repair and editing. However, pAgos have the distinct advantage of not requiring a  
35 protospacer adjacent motif (PAM) for function<sup>2-5</sup>, which means that pAgos are not limited to targets flanked  
36 by PAM sites and can potentially cut any DNA target regardless of composition. Despite this potential, no  
37 pAgo has been developed that rivals the simplicity and function of Cas9-based strategies.

38 Long pAgos are predicted to serve as a form of adaptive defense against invading nucleic acids such as  
39 phage/viral DNA and RNA<sup>6,7</sup>. With a single-stranded DNA and/or RNA as a guide, long pAgos cleave  
40 complementary target DNA, RNA, or both via the conserved catalytic tetrad, DEDX<sup>1</sup>. To create a double-  
41 stranded DNA break, long pAgos require two guides. Target recognition and cleavage is enabled by four  
42 canonical domains<sup>3</sup>: N (N-terminal), PAZ (PIWI-Argonaute-Zwille), MID (middle), and PIWI (P element-  
43 induced wimpy testis). The N-terminal domain is essential in target cleavage<sup>8,9</sup> and dissociation of cleaved  
44 strands<sup>9,10</sup>, though the detailed mechanism remains poorly understood. The MID domain interacts with the  
45 5'-end of the guide<sup>11</sup> and promotes binding of the guide to its target nucleic acids<sup>12</sup>. The PAZ domain  
46 interacts with the 3' end of a guide<sup>13-16</sup>, protecting it from degradation<sup>17</sup>. The PIWI domain plays a pivotal  
47 role in nucleic acid cleavage via the conserved catalytic tetrad, DEDX (D: aspartate, E: glutamate, X:  
48 histidine, aspartate or asparagine)<sup>6</sup>. Despite the presence of these canonical domains in all long pAgos,  
49 currently characterized pAgos including TtAgo<sup>2</sup>, MpAgo<sup>5</sup>, PfAgo<sup>18</sup> and MjAgo<sup>3,19</sup> work at very high  
50 temperatures (>55 °C)<sup>2,3,5,18</sup>, making them infeasible for gene editing in common mesophilic organisms.

51 The halophilic Argonaute from *Natronobacterium gregoryi* (NgAgo) was recently put forth as a promising  
52 candidate for pAgo-mediated gene editing as it is believed to operate at mesophilic (~37°C) temperatures<sup>20</sup>.  
53 However, these claims have since been refuted due to an inability to demonstrate *in vitro* DNA cleavage or  
54 to replicate these findings in a number of eukaryotic hosts<sup>21-25</sup>. NgAgo expression is poor, presumably due  
55 to its halophilic characteristics that make low salt expression challenging<sup>26,27</sup>. Thus, all published *in vitro*  
56 cleavage assays have relied on refolded protein<sup>21-25</sup>, which may be non-functional, resulting in the  
57 inconclusive results. Nonetheless, recent work by Fu and colleagues demonstrated that NgAgo may still  
58 have potential as a gene editor for prokaryotic hosts. While the authors were able to confirm that gene-  
59 editing was mediated by homologous recombination via RecA, which physically associated with NgAgo in  
60 an unanticipated manner, the specific role of NgAgo remained unclear. Here, we demonstrate that NgAgo  
61 is indeed a DNA endonuclease by identifying a catalytic mutant that is required for DNA cleavage, and  
62 provide evidence that this activity is essential for NgAgo-mediated gene editing via homologous  
63 recombination repair.

## 64 MATERIAL AND METHODS

## 65 **Strains and plasmids**

66 *E. coli* strains and plasmids used in this study are listed in Table 1. Cloning was carried out according to  
67 standard practices<sup>28</sup> with primers, template, and purpose listed in Supplementary Table 1. Plasmids were  
68 maintained in *E. coli* DH5 $\alpha$ . NgAgo variants (wildtype, D663A/D738A, N-del, and repA with GST or His tag)  
69 that were used for *in vitro* activity assays were cloned into a IPTG-inducible T7 plasmid via the pET32a-  
70 GST-ELP64 (provided by Professor Xin Ge, University of California, Riverside).

71 To test the homologous recombination ability of NgAgo, we cloned pTKDP-KanR-mNeonGreen-hph for  
72 recombineering and made p15-KanR-PtetRed as our donor plasmid with inducible lambda-red  
73 recombinase (Table 1).

## 74 **NgAgo expression and purification**

75 All GST-NgAgo or His-NgAgo variants were transformed into BL21 (DE3) electrocompetent cells and were  
76 plated on agar plates containing ampicillin (100  $\mu$ g/ml). A single colony was inoculated in LB with ampicillin  
77 for 16 hours and then cultured in 100 ml of LB containing ampicillin. Expression was induced with IPTG at  
78 0.1 mM final concentration when the culture OD600 reached 0.5. After 4 hours incubation at 37 °C or 22  
79 °C overnight, cells were collected by centrifuge 7500 rpm at 4 °C for 5 minutes. The cell pellet was  
80 resuspended in TN buffer (10 mM Tris and 100mM NaCl, pH 7.5) and lysed via sonication at a medium  
81 power setting (~50 W) in 10 s intervals, with intervening 10 s incubations on ice to reduce heat denaturation.  
82 Cell lysates were then clarified at 12000 rpm at 4 °C for 30 minutes. The supernatant was collected as a  
83 soluble protein fraction. Both soluble and insoluble (cell pellet) fractions were purified via His-IDA nickel  
84 column (Clontech Laboratories, Mountain View, CA. Cat. No: 635657) according to the manufacturer  
85 instructions. Insoluble NgAgo protein was refolded on the column after denaturation with guanidium chloride  
86 according to manufacturer instructions. GST-tagged NgAgo variants were purified by glutathione agarose  
87 (Thermo Fisher Scientific, Waltham, MA. Cat. No: 16100) according to the manufacturer protocol.

## 88 ***In vitro* activity assay**

89 For the reloading protocol, five micrograms of purified NgAgo were mixed with one microgram total of  
90 phosphorylated single-stranded DNA (P-ssDNA) targeting mNeonGreen (Supplementary Table 2) and  
91 incubated at 55 °C for an hour. 200-300 ng of substrate plasmid DNA (pNCS-mNeonGreen) was then  
92 added to the sample. The final volume of the reaction was 50  $\mu$ l (working concentration: 20 mM Tris-Cl,  
93 300 mM KCl, 500  $\mu$ M MgCl<sub>2</sub>, and 2 mM DTT). The sample was then incubated at 37 °C for three hours. 0.8  
94 units of Proteinase K (NEB, Ipswich, MA. Cat. No: P8107S) were added to the sample to digest the protein  
95 for 5 minutes at 37 °C. The nucleic acids were then cleaned up by the DNA Clean & Concentrator™-5 kit  
96 (Zymo Research, Irvine, CA. Cat. No: D4003T) according to manufacturer instructions and mixed with 6X  
97 loading dye containing SDS (Thermo Fisher S, Waltham, MA. Cat. No: R1151) before gel electrophoresis.

98 The gel containing Sybrsafe (Thermo Fisher S, Waltham, MA. Cat. No: S33102) was visualized under a  
99 blue light (Azure Biosystems, Dublin, CA. Azure c400).

100 For our standard protocol, we incubated the same amount of guides and proteins at 37 °C for 30 minutes,  
101 and added the same amount of plasmid DNA (p15-KanR or pBSI-Scel(E/H)<sup>31</sup>) with 50 ul final volume  
102 (working concentration: 20mM Tris-Cl, 300mM NaCl, 250 uM MgCl<sub>2</sub>, and 2mM DTT). The samples were  
103 incubated at 37 °C for an hour before Proteinase K treatment. The rest of the procedure is the same as the  
104 reloading protocol.

105 As positive controls for nicked and linearized DNA, we digested plasmid pBSI-Scel(E/H) with I-Scel or a  
106 K223I I-Scel mutant<sup>31</sup>, generating linearized and nicked DNA, respectively. We tested five micrograms of  
107 each NgAgo variant with pBSI-Scel(E/H) and conducted electrophoresis to check the plasmid conformation.  
108 To exclude the possibility of band shift due to DNA binding, we treated the samples with 0.8 units of  
109 proteinase K and used a gel loading dye with SDS when running on a gel.

#### 110 **Electrophoretic mobility shift assay (EMSA)**

111 Five microgram of purified N-del and repA were incubated with one microgram of mNeonGreen ssDNA  
112 guide in 50ul in buffer (working concentration: 20 mM Tris-Cl, 300 mM KCl, 500 μM MgCl<sub>2</sub>, and 2 mM DTT)  
113 at 37°C for an hour and treated with 0.8 units proteinase K for 5 minutes if needed before running with 20%  
114 TBE gel with 0.5X TBE buffer. Gels were stained with Sybr Gold (Thermo Fisher Scientific, Waltham, MA.  
115 Cat. No: S11494) before visualizing under a green fluorescent channel (Azure Biosystems, Dublin, CA.  
116 Azure c400). Positional marker 10/60 ladder (Coralville, IA. Cat. No: 51-05-15-01) was used in the EMSA  
117 assay.

#### 118 **Gene-editing assay**

119 MG1655 (DE3) *atpI::KanR-mNeonGreen* was transformed with pET-GST-NgAgo-His (to induce DNA  
120 cleavage) and p15-KanR-PtetRed (for lambda-red recombinase expression and to provide donor DNA for  
121 repair) and made electrocompetent. Electrocompetent cells were transformed with either no guides or one  
122 microgram total of FW, RV, both guides and incubated in Miller LB with ampicillin, chloramphenicol, and  
123 IPTG for an hour. These cultures were then diluted ten-fold in Miller LB containing ampicillin (working  
124 concentration: 100 μg/ml), chloramphenicol (working concentration: 25 μg/ml), IPTG (working  
125 concentration: 0.1mM), and anhydrotetracycline (aTc) (working concentration: 50 μg/ml), incubated for 2  
126 hours before plating with and without kanamycin. Colony forming units (CFU) were counted after 16-20  
127 hours incubation at 37 °C. The unguided control was normalized to 100% and guided-treatments were  
128 normalized to the unguided control.

#### 129 **Phyre 2 and HHpred analysis**

130 NgAgo protein (IMG/M Gene ID: 2510572918) was analyzed via Phyre 2<sup>34</sup> with normal mode on 2018  
131 November 19. The normal mode pipeline involves detecting sequence homologues, predicting secondary  
132 structure and disorder, constructing a hidden Markov model (HMM), scanning produced HMM against  
133 library of HMMs of proteins with experimentally solved structures, constructing 3D models of NgAgo,  
134 modelling insertions/deletions, modelling of amino acid sidechains, submission of the top model, and  
135 transmembrane helix and topology prediction<sup>34</sup>. NgAgo was analyzed via HHpred<sup>35</sup>  
136 (<https://toolkit.tuebingen.mpg.de/#/tools/hhpred>) on 2018 November 27. The parameters for HHpred are  
137 HHblits=>uniclust30\_2018\_08 for multiple sequence alignment (MSA) generation method, 3 for maximal  
138 number of MSA generation steps, 1e-3 for E-value incl. threshold for MSA generation, 0% for minimum  
139 sequence identity of MSA hits with query, 20% for minimum coverage of MSA hits, during\_alignment for  
140 secondary structure scoring, local for alignment mode, off for realign with MAC, 0.3 for MAC realignment  
141 threshold, 250 for number of target sequences, and 20% for minimum probability in hit list.

## 142 **Phylogenetic analysis**

143 BLAST was used to compare NgAgo protein sequence with all the isolates in the database via the IMG/M  
144 server (<https://img.jgi.doe.gov/>). Representative full-length Argonautes with a repA domain were used to  
145 represent each species. Selected pAgos with repA domains and some well-characterized pAgos were  
146 compared, and the midpoint rooted tree was generated via the server <http://www.genome.jp/tools-bin/ete>  
147 with unaligned input type, mafft\_default aligner, no alignment cleaner, no model tester, and fasttree\_default  
148 Tree builder parameters. The nwk output file was then used for phylogenetic tree generation in R with  
149 ggtree package.

## 150 **RESULTS**

### 151 **NgAgo has canonical N-terminal, PIWI, MID, and PAZ domains, and a putative single stranded DNA** 152 **binding (repA) domain.**

153 Given the ongoing debate of the function of NgAgo, we analysed its sequence (IMG/M Gene ID:  
154 2510572918) with Phyre 2<sup>34</sup> and HHpred<sup>36</sup> to predict its structure based on characterized structural  
155 homologs. Phyre 2 and HHpred analyses found with high confidence (probability = 100%) that NgAgo  
156 shares structural features with catalytically active pAgos and eukaryotic Agos (eAgos) including archaeal  
157 MjAgo, bacterial TtAgo, and eukaryotic hAgo2 (Supplementary Table 3 and 4). Since MjAgo is the only  
158 characterized pAgo from Archaea, we used it as a template for comparative modelling. The predicted  
159 NgAgo structure is similar to the crystal structure of MjAgo, consisting of canonical N-terminal, PAZ, MID,  
160 and PIWI domains (100% probability in both Phyre 2 and HHpred) (Fig. 1a and b). However, the N-terminal  
161 domain of NgAgo is truncated, relative to MjAgo, potentially suggesting a novel mechanism for strand  
162 displacement and binding due to the N-terminal domain's role in pAgo targeted cleavage.

163 Structural analysis also identified an uncharacterized oligonucleotide/oligosaccharide-binding (OB) fold  
164 domain between residues 13-102 of NgAgo that is known to bind single-stranded DNA in eukaryotes and  
165 prokaryotes<sup>37</sup> (Fig. 1b). This OB domain has recently been identified as a new feature of pAgos<sup>38</sup>. As repA  
166 proteins were the most common matches on both Phyre 2 and HHpred, we will refer to this OB domain as  
167 repA (Supplementary Tables 5 and 6). While the repA domain is absent in all characterized pAgos, at least  
168 12 Ago homologs from various species deposited on IMG/M (<https://img.jgi.doe.gov/>) share this domain.  
169 Phylogenetic analysis showed that all the repA-containing pAgos were from halophilic Archaea forming a  
170 clade that is distinct from that of the current well-characterized pAgos (Fig. 1c). This monophyletic group of  
171 repA-containing pAgos may represent a new class of pAgos that is currently unrecognized in the literature<sup>39</sup>.  
172 Moreover, its unique presence within halophiles suggests that the repA domain may be required for function  
173 in high salt environments, potentially replacing the role of the canonical N-terminal domain, which was then  
174 truncated through evolution.

175 Our analysis of NgAgo also confirmed the presence of a conserved catalytic tetrad, DEDX (X: H, D or N)<sup>6</sup>,  
176 which is critical for nucleic acid cleavage by the PIWI domain of Argonautes. The catalytic tetrad (D663,  
177 E704, D738, and D863) of NgAgo aligns well with those from other catalytically active pAgos, including  
178 MjAgo<sup>3</sup>, PfAgo<sup>18</sup>, MpAgo<sup>5</sup>, and TtAgo<sup>2</sup> (Fig. 1d). Moreover, structural alignment of NgAgo and MjAgo  
179 display good colocalization of the catalytic tetrad, except for E704, suggesting that NgAgo may have similar  
180 nucleic acid cleavage activity (Fig. 1e).

### 181 **Soluble but not refolded NgAgo exhibits random DNA cleavage activity *in vitro***

182 As halophilic proteins tend to be insoluble when expressed in a low-salt environment due to their sequence  
183 adaptations<sup>26,27,40</sup>, we first optimized expression conditions to obtain more soluble NgAgo protein  
184 (Supplementary Fig. 1). We purified wildtype NgAgo (Fig. 2a) from both the soluble and insoluble fractions  
185 to test for guide-dependent DNA cleavage using 5'P-ssDNA as guides. Insoluble NgAgo was refolded  
186 during purification using a previously published method<sup>41</sup>. Our results showed that purified NgAgo from the  
187 soluble cell lysate fraction (sNgAgo) nicks plasmid DNA and genomic DNA, independent of guide (Fig. 2b  
188 and supplementary Fig. 2e), as evidenced by the presence of the nicked and linearized plasmid. However,  
189 purified refolded NgAgo from the insoluble lysate fraction (rNgAgo) has little or no activity on DNA (Fig. 2c),  
190 consistent with a study by Ye and colleagues<sup>41</sup>. We hypothesized that NgAgo generates random guides in  
191 the host via DNA chopping<sup>42</sup>, which co-purifies with NgAgo leading to apparent guide-independent activity  
192 *in vitro*. While we were able to confirm the presence of these random copurified guides (Fig. 2d), we were  
193 unable to displace them with incubation at high temperature (55 °C) and reload with our target guides  
194 (reloading protocol). Subsequent testing had similar guide-independent cleavage activity with no evidence  
195 of increased linearized plasmid (Supplementary Fig. 3). As refolded NgAgo had no cleavage activity, we  
196 used soluble NgAgo to study its function *in vitro* unless otherwise stated.



197 Previous studies have demonstrated that TtAgo can obtain random guides from the expression plasmid  
198 DNA via DNA chopping<sup>2</sup>. Thus, the observed guide-independent cleavage may indeed be guide-dependent  
199 as a result of chopping and subsequent guide loading with homologous DNA, which cannot be easily  
200 displaced as demonstrated in Fig 2c. To examine this hypothesis, we completed the *in vitro* cleavage assay  
201 with a 'related' plasmid, pNCS-mNeonpGreen (Supplementary Fig. 2a), and an 'unrelated' plasmid, p15-  
202 KanR (Supplementary Fig. 2c). The unrelated plasmid, p15-KanR, shares no DNA homology with the  
203 NgAgo expression plasmid while the related plasmid, pNCS-mNeonGreen, has the same ampicillin  
204 resistance gene. NgAgo cleaved both related and unrelated plasmids independent of guide (Supplementary  
205 Fig. 2b and 2d), suggesting that the guide-independent cleavage activity of our purified NgAgo does not  
206 rely on pre-loaded DNA. These results confirmed that NgAgo has guide-independent cleavage activity *in*  
207 *vitro*, sharing similar properties with bacterial TtAgo<sup>42</sup> and archaeal MjAgo<sup>19</sup>.

### 208 **RepA and PIWI domains are responsible for NgAgo DNA cleavage**

209 As NgAgo cuts plasmids independent of guide, we used this activity to identify which domains are  
210 responsible for DNA cleavage. Since *in silico* analysis identified an uncharacterized repA domain, we  
211 constructed a repA mutant (residues 1-102) and a repA-deletion (residues 105-887, referred to as N-del)  
212 (Fig. 2a) to examine whether repA is required for NgAgo function. We also constructed double mutants,  
213 D663A/D738A, containing mutations at putative active site residues (this double mutant corresponds to the  
214 catalytic double mutant, D478A/D546A, of TtAgo<sup>2</sup> that loses all cleavage activities<sup>2,42</sup>) in the full-length  
215 protein and N-del (Fig. 2a). *In vitro* cleavage assays with repA confirm that it nicks and cleaves plasmid  
216 DNA, as evidenced by open-circular and linearized plasmid (Fig. 2e). Although the repA domain is able to  
217 bind to ssDNA as demonstrated on an electrophoretic mobility shift assay (EMSA) (Fig. 2c), the mechanism  
218 by which it cuts DNA remains unknown.

219 Our cleavage assays with NgAgo mutants suggest that multiple domains are involved in NgAgo activity  
220 (Fig. 2e). An N-del truncation mutant that lacks the repA domain displays cleavage activity. Similarly,  
221 D663A/D863A mutants containing mutations in the canonically catalytic PIWI domain maintain similar  
222 guide-independent nicking and cleaving activity relative to wildtype. Thus, repA and PIWI domains appear  
223 to both cut DNA independently from one another and can complement the loss of function from the other.  
224 Indeed, mutants containing combined mutations (N-del/D663A/D863A) lose all ability to nick/linearize  
225 plasmids (Fig. 2e), suggesting that the nicking/cleaving activities of N-del is dependent on the putative  
226 catalytic tetrad within the PIWI domain (Fig. 1d and 1e). Collectively, our work shows that NgAgo is a DNA  
227 endonuclease, dependent on the function of its repA and PIWI domains.

### 228 **repA and PIWI domains are essential for programmable DNA editing**

229 Since we have shown that NgAgo can cleave DNA, and since work from other groups indicated the protein  
230 is active *in vivo*<sup>43</sup>, we asked if NgAgo can be repurposed as a guided gene-editing tool in *E.coli*. We chose

231 *E.coli* instead of mammalian cells as our model because *E.coli* lacks histones, which are known to inhibit  
232 pAgo activity<sup>19</sup>. To test for NgAgo gene editing activity, we created an MG1655 (DE3) strain harbouring a  
233 cassette composed of a *kanR* gene and a *mNeonGreen* gene lacking an RBS and promoter, flanked by  
234 two double terminators (Fig. 3a). This arrangement prevents any KanR/mNeonGreen expression from  
235 transcription read-through and translation from upstream and downstream genes. Since DNA breaks in  
236 *E.coli* are lethal, only correct recombinants will survive on kanamycin plates when provided with donor  
237 plasmid, which harbors a truncated *mNeonGreen*, a constitutive promoter, an RBS and a truncated *kanR*  
238 (Fig. 3a). We then demonstrated that ssDNA could survive long enough to form a complex with NgAgo  
239 before degradation (Supplementary Fig. 4). Wildtype NgAgo increased homologous recombination  
240 efficiency 107%, 82%, and 31% when provided with FW, RV, and both guides, respectively, compared with  
241 an unguided control (Fig. 3b), demonstrating that guide-dependent NgAgo activity can enhance gene  
242 editing.

243 Given that the PIWI domain is essential for guide-dependent cleavage activity in other studied pAgos<sup>2,5,18</sup>,  
244 we tested its essentiality for homologous recombination in NgAgo. The PIWI mutant, D663A/D738A, of  
245 NgAgo demonstrated a statistically significant enhancement in homologous recombination; however, this  
246 was roughly half of what was seen in the wildtype protein (43% above no guide controls). The PIWI mutant  
247 displayed no significant enhancement of recombination with the FW or both guides (Fig. 3b). While the  
248 mechanism behind this pattern is unclear, these data suggest that the PIWI domain is not essential for  
249 guide-dependent cleavage activity of NgAgo.

250 Additionally, as the repA domain is not common amongst pAgos, we tested if it was required for DNA  
251 targeting activity. The N-del mutant of NgAgo lacking the repA domain displayed only an 11% enhancement  
252 in homologous recombination above unguided controls in the presence of the RV guide only (Fig. 3b).  
253 Nonetheless, this is consistent with a mechanism in which repA also plays a role in guide-dependent  
254 cleavage activity. Consistent with *in vitro* results, an N-del/D663A/D738A catalytic mutant showed no  
255 increase in gene editing activity in the presence of FW, RV, or both guides compared to an unguided control.  
256 Thus, the DNA endonuclease activity mediated by the repA and PIWI domains is essential for enhanced  
257 homologous recombination and gene editing.

## 258 **DISCUSSION**

### 259 **NgAgo may represent a new class of mesophilic pAgos**

260 To our knowledge, NgAgo is the first studied pAgo with an uncharacterized repA domain, which indeed  
261 binds to single-stranded DNA (Fig. 2f). Surprisingly, we found that repA alone contributes to DNA cleavage  
262 activity (Fig. 2e). Moreover, repA aids the PIWI domain in NgAgo targeted DNA cleavage as homologous  
263 recombination is reduced in N-del mutants relative to wildtype (Fig. 3). Interestingly, all repA domain-  
264 containing pAgos are from halophilic Archaea mesophiles, suggesting that the repA domain may be



265 required for pAgos to function in high-salt environments. Given that *Natronobacterium gregoryi*, the native  
266 host of NgAgo, is a halophile, the protein must have evolved ways to maintain protein-DNA interactions for  
267 catalysis in high salt environments where many electrostatic interactions are reduced. As demonstrated by  
268 Hunt and co-workers, single-stranded binding (SSB) protein enhances TtAgo activity<sup>44</sup>; repA at the N-  
269 terminus of NgAgo may be involved in the cleaving process without recruiting SSB protein. Moreover, as  
270 the N-terminal domain of pAgos is essential for target cleavage<sup>6</sup>, repA may supplant its role resulting in the  
271 truncated N-terminal domain of NgAgo. Further research, however, is needed to clarify the function of this  
272 repA domain.

### 273 **NgAgo is a DNA-guided DNA endonuclease**

274 Although previous studies demonstrated that refolded NgAgo does not cut DNA *in vitro*<sup>41,44</sup>, consistent with  
275 our findings, we establish that soluble NgAgo can, in fact, cleave DNA *in vitro*. That is, refolded NgAgo may  
276 not be fully functional. As we showed that an N-del/D663A/D738A catalytic mutant lacks DNA cleaving  
277 activity (Fig. 2e), the catalytic activity is unlikely to be the result of sample contamination. However, we are  
278 unable to demonstrate unequivocal guide-dependent cleavage with both double-stranded DNA target and  
279 single-stranded DNA target *in vitro* (data not shown). This may be due to inefficient guide loading, as we  
280 observe that N-del co-purifies guides (Fig. 2c).

### 281 **NgAgo can be repurposed as a DNA editing tool**

282 Our results provide supporting evidence to encourage the development of NgAgo for gene-editing. When  
283 provided with homologous target regions, NgAgo can aid in homologous recombination. Much like other  
284 pAgos, the PIWI domain participates in DNA editing as shown here and by Fu *et al.* Moreover, without  
285 repA, PIWI mutants of NgAgo exhibit reduced cleavage activity with a concomitant reduction in homologous  
286 recombination efficiency. Both the repA deletion and the PIWI mutation (N-del/D663A/D738) are needed  
287 to fully abolish catalytic and gene editing functions. Thus, in the presence of both functional domains,  
288 NgAgo can effectively enhance homologous recombination by inducing a double stranded break at a  
289 targeted region. Despite the programmable DNA-cleaving ability of NgAgo, there remains several  
290 challenges to its development as a robust tool for gene-editing applications: high off-target activity or guide  
291 independent cleavage, poor expression, and potentially low activity in eukaryotic hosts. Nonetheless,  
292 further insight may lead to protein engineering strategies to overcome these hurdles and develop NgAgo  
293 as a robust tool for gene-editing.

### 294 **Conclusion**

295 Based on the above findings, we conclude that NgAgo is a novel DNA endonuclease that belongs to an  
296 unrecognized class of pAgos defined by a characteristic repA domain. NgAgo cleaves DNA through both a  
297 well-conserved catalytic tetrad in PIWI and through a novel uncharacterised repA domain. This cleavage

298 activity is essential to enhancing gene-editing efficiency in prokaryotes. Despite the challenges of NgAgo,  
299 our work provides insight into poorly characterized NgAgo for subsequent gene-editing tool development,  
300 and sheds new light on seemingly contradictory reports.

#### 301 **FUNDING**

302 This research was supported by the startup funds from the Colleges of Engineering and Agriculture, and  
303 the USDA National Institute of Food and Agriculture (Hatch Multistate Project S1041).

#### 304 **Acknowledgment**

305 We are grateful to Dr. Xin Ge (University of California, Riverside) and Dr. Kristala J. Prather (Massachusetts  
306 Institute of Technology) for providing pET32a-GST-ELP64 plasmid and MG1655 (DE3), respectively. We  
307 also thank Dr. Mathew Tantama (Purdue University) for providing pBAD-mTagBFP2 plasmid.

#### 308 **CONFLICT OF INTEREST**

309 K.V.S., K.Z.L., and M.A.M. have filed a patent related to this work.

#### 310 **Author contributions**

311 K.V.S. and K.Z.L. designed the experiments. K.Z.L., M.A.M., A.K., A.L., and P.P. conducted and analyzed  
312 the experiments. K.V.S., F.G., and K.Z.L. supervised research and experimental design. K.V.S, K.Z.L,  
313 M.A.M, and F.G. wrote the manuscript.

314

315 **References**

- 316 1. Hegge, J. W., Swarts, D. C. & van der Oost, J. Prokaryotic Argonaute proteins: novel genome-editing  
317 tools? *Nature Reviews Microbiology* **16**, 5 (2018).
- 318 2. Swarts, D. C. *et al.* DNA-guided DNA interference by a prokaryotic Argonaute. *Nature* **507**, 258-261  
319 (2014).
- 320 3. Willkomm, S. *et al.* Structural and mechanistic insights into an archaeal DNA-guided Argonaute protein.  
321 *Nature Microbiology* **2**, 17035 (2017).
- 322 4. Enghiad, B. & Zhao, H. Programmable DNA-guided artificial restriction enzymes. *ACS synthetic biology*  
323 **6**, 752-757 (2017).
- 324 5. Kaya, E. *et al.* A bacterial Argonaute with noncanonical guide RNA specificity. *Proceedings of the*  
325 *National Academy of Sciences* **113**, 4057-4062 (2016).
- 326 6. Swarts, D. C. *et al.* The evolutionary journey of Argonaute proteins. *Nature structural & molecular*  
327 *biology* **21**, 743-753 (2014).
- 328 7. Koonin, E. V. Evolution of RNA-and DNA-guided antiviral defense systems in prokaryotes and  
329 eukaryotes: common ancestry vs convergence. *Biology direct* **12**, 5 (2017).
- 330 8. Hauptmann, J. *et al.* Turning catalytically inactive human Argonaute proteins into active slicer enzymes.  
331 *Nature Structural and Molecular Biology* **20**, 814 (2013).
- 332 9. Faehnle, C. R., Elkayam, E., Haase, A. D., Hannon, G. J. & Joshua-Tor, L. The making of a slicer:  
333 activation of human Argonaute-1. *Cell reports* **3**, 1901-1909 (2013).
- 334 10. Kwak, P. B. & Tomari, Y. The N domain of Argonaute drives duplex unwinding during RISC assembly.  
335 *Nature structural & molecular biology* **19**, 145 (2012).
- 336 11. Ma, J.-B. *et al.* Structural basis for 5'-end-specific recognition of guide RNA by the *A. fulgidus* Piwi  
337 protein. *Nature* **434**, 666 (2005).
- 338 12. Künne, T., Swarts, D. C. & Brouns, S. J. J. Planting the seed: target recognition of short guide RNAs.  
339 *Trends in microbiology* **22**, 74-83 (2014).
- 340 13. Lingel, A., Simon, B., Izaurralde, E. & Sattler, M. Nucleic acid 3'-end recognition by the Argonaute2  
341 PAZ domain. *Nature Structural and Molecular Biology* **11**, 576 (2004).
- 342 14. Ma, J.-B., Ye, K. & Patel, D. J. Structural basis for overhang-specific small interfering RNA recognition  
343 by the PAZ domain. *nature* **429**, 318 (2004).
- 344 15. Sheng, G. *et al.* Structure-based cleavage mechanism of *Thermus thermophilus* Argonaute DNA guide  
345 strand-mediated DNA target cleavage. *Proceedings of the National Academy of Sciences* **111**, 652-  
346 657 (2014).
- 347 16. Wang, Y. *et al.* Structure of an argonaute silencing complex with a seed-containing guide DNA and  
348 target RNA duplex. *nature* **456**, 921 (2008).
- 349 17. Hur, J. K., Zinchenko, M. K., Djuranovic, S. & Green, R. Regulation of Argonaute slicer activity by guide  
350 RNA 3'end interactions with the N-terminal lobe. *Journal of Biological Chemistry*, jbc-M112 (2013).

- 351 18. Swarts, D. C. *et al.* Argonaute of the archaeon *Pyrococcus furiosus* is a DNA-guided nuclease that  
352 targets cognate DNA. *Nucleic acids research* **43**, 5120-5129 (2015).
- 353 19. Zander, A. *et al.* Guide-independent DNA cleavage by archaeal Argonaute from *Methanocaldococcus*  
354 *jannaschii*. *Nature Microbiology* **2**, 17034 (2017).
- 355 20. Cyranoski, D. Authors retract controversial NgAgo gene-editing study. *Nature News*,  
356 doi:10.1038/nature.2017.22412 (2017).
- 357 21. Javidi-Parsijani, P. *et al.* No evidence of genome editing activity from *Natronobacterium gregoryi*  
358 Argonaute (NgAgo) in human cells. *Plos One* **12**, 14, doi:10.1371/journal.pone.0177444 (2017).
- 359 22. Wu, Z. *et al.* NgAgo-gDNA system efficiently suppresses hepatitis B virus replication through  
360 accelerating decay of pregenomic RNA. *Antiviral Research* (2017).
- 361 23. Burgess, S. *et al.* Questions about NgAgo. *Protein & Cell* **7**, 913-915, doi:10.1007/s13238-016-0343-9  
362 (2016).
- 363 24. Khin, N. C., Lowe, J. L., Jensen, L. M. & Burgio, G. No evidence for genome editing in mouse zygotes  
364 and HEK293T human cell line using the DNA-guided *Natronobacterium gregoryi* Argonaute (NgAgo).  
365 *PloS one* **12**, e0178768 (2017).
- 366 25. Qin, Y. Y., Wang, Y. M. & Liu, D. NgAgo-based fabp11a gene knockdown causes eye developmental  
367 defects in zebrafish. *Cell Research* **26**, 1349-1352, doi:10.1038/cr.2016.134 (2016).
- 368 26. Elcock, A. H. & McCammon, J. A. Electrostatic contributions to the stability of halophilic proteins.  
369 *Journal of molecular biology* **280**, 731-748 (1998).
- 370 27. Tadeo, X. *et al.* Structural basis for the aminoacid composition of proteins from halophilic archaea. *PLoS*  
371 *biology* **7**, e1000257 (2009).
- 372 28. Sambrook, J., Fritsch, E. F. & Maniatis, T. *Molecular cloning: a laboratory manual*. (Cold spring harbor  
373 laboratory press, 1989).
- 374 29. Wood, W. B. Host specificity of DNA produced by *Escherichia coli*: bacterial mutations affecting the  
375 restriction and modification of DNA. *Journal of molecular biology* **16**, 118-IN113 (1966).
- 376 30. Tseng, H.-C., Martin, C. H., Nielsen, D. R. & Prather, K. L. J. Metabolic engineering of *Escherichia coli*  
377 for enhanced production of (R)- and (S)-3-hydroxybutyrate. *Applied and environmental microbiology* **75**,  
378 3137-3145 (2009).
- 379 31. Niu, Y., Tenney, K., Li, H. & Gimble, F. S. Engineering variants of the I-SceI homing endonuclease with  
380 strand-specific and site-specific DNA-nicking activity. *Journal of molecular biology* **382**, 188-202 (2008).
- 381 32. Rhodius, V. A. *et al.* Design of orthogonal genetic switches based on a crosstalk map of  $\sigma_s$ , anti- $\sigma_s$ ,  
382 and promoters. *Molecular systems biology* **9**, 702 (2013).
- 383 33. Reisch, C. R. & Prather, K. L. J. The no-SCAR (Scarless Cas9 Assisted Recombineering) system for  
384 genome editing in *Escherichia coli*. *Scientific reports* **5**, 15096 (2015).
- 385 34. Kelley, L. A., Mezulis, S., Yates, C. M., Wass, M. N. & Sternberg, M. J. E. The Phyre2 web portal for  
386 protein modeling, prediction and analysis. *Nature protocols* **10**, 845-858 (2015).

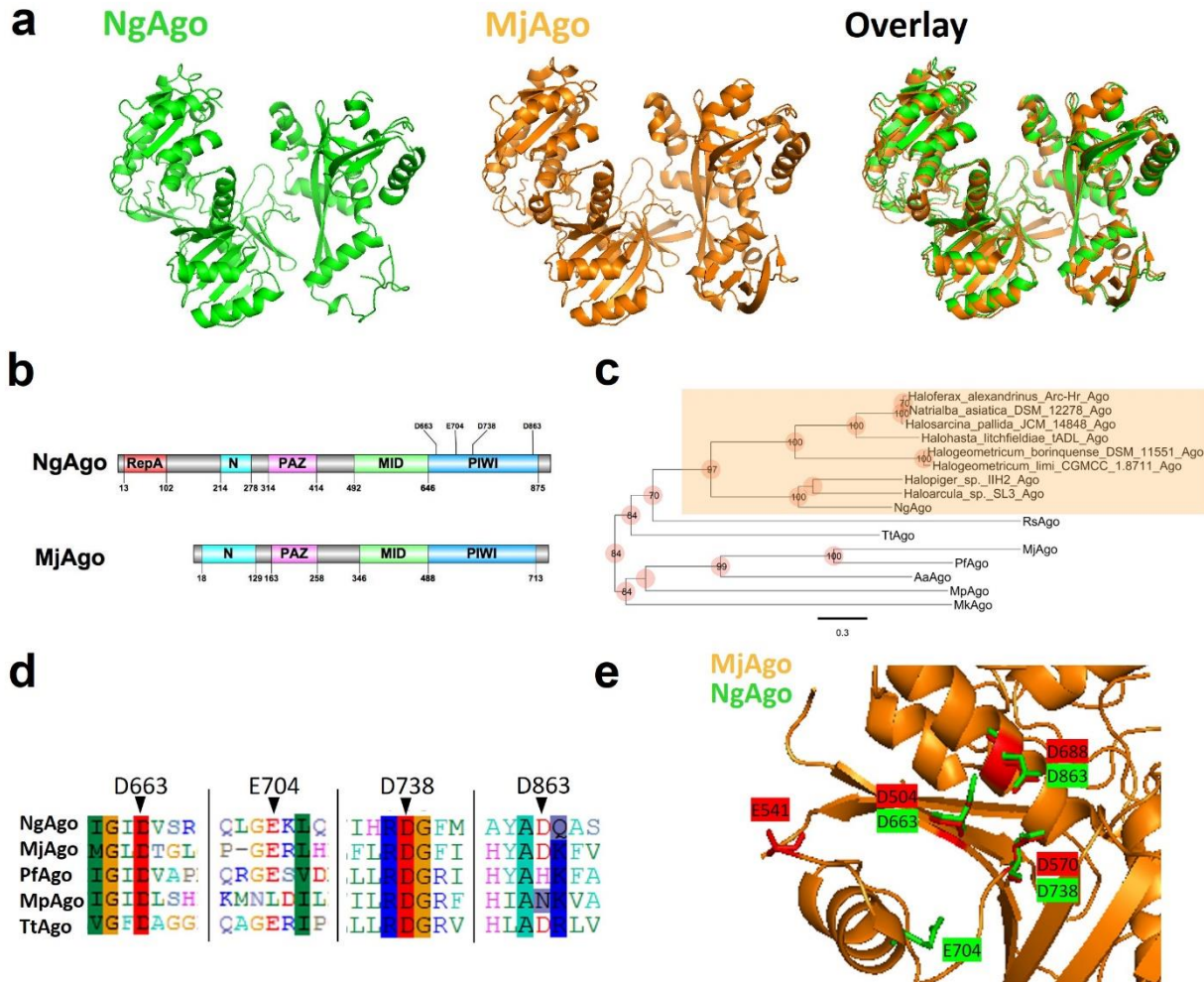
- 387 35. Zimmermann, L. *et al.* A completely Reimplemented MPI bioinformatics toolkit with a new HHpred  
388 server at its Core. *Journal of molecular biology* **430**, 2237-2243 (2018).
- 389 36. Söding, J., Biegert, A. & Lupas, A. N. The HHpred interactive server for protein homology detection  
390 and structure prediction. *Nucleic acids research* **33**, W244-W248 (2005).
- 391 37. Flynn, R. L. & Zou, L. Oligonucleotide/oligosaccharide-binding fold proteins: a growing family of  
392 genome guardians. *Critical reviews in biochemistry and molecular biology* **45**, 266-275 (2010).
- 393 38. Ryazansky, S., Kulbachinskiy, A. & Aravin, A. The expanded universe of prokaryotic Argonaute  
394 proteins. *bioRxiv*, 366930 (2018).
- 395 39. Ryazansky, S., Kulbachinskiy, A. & Aravin, A. A. The expanded universe of prokaryotic Argonaute  
396 proteins. *mBio* **9**, e01935-01918 (2018).
- 397 40. Müller-Santos, M. *et al.* First evidence for the salt-dependent folding and activity of an esterase from  
398 the halophilic archaea *Haloarcula marismortui*. *Biochimica et Biophysica Acta (BBA)-Molecular and*  
399 *Cell Biology of Lipids* **1791**, 719-729 (2009).
- 400 41. Sunghyeok, Y. *et al.* DNA-dependent RNA cleavage by the *Natronobacterium gregoryi* Argonaute.  
401 *BioRxiv*, 101923 (2017).
- 402 42. Swarts, D. C. *et al.* Autonomous Generation and Loading of DNA Guides by Bacterial Argonaute.  
403 *Molecular Cell* **65**, 985-998 (2017).
- 404 43. Fu, L. *et al.* The prokaryotic Argonaute proteins enhance homology sequence-directed recombination  
405 in bacteria. *Nucleic acids research* (2019).
- 406 44. Hunt, E. A., Evans Jr, T. C. & Tanner, N. A. Single-stranded binding proteins and helicase enhance the  
407 activity of prokaryotic argonautes in vitro. *PloS one* **13**, e0203073 (2018).

408 

409

410

411 FIGURES



412

413

414 **Figure 1 | NgAgo belongs to a distinct clade of pAgos with a catalytic DEDX tetrad and novel repA**

415 **domain.** **a**, Phyre 2 simulation 3D structure based on MjAgo structure (PDB: 5G5T). NgAgo structure is

416 similar to the MjAgo structure except for the N-terminal domain. **b**, Domain architecture of NgAgo based on

417 Phyre2 and HHpred reveals that NgAgo has an uncharacterized repA domain, a truncated N-terminal

418 domain, a MID domain, and a PIWI domain. **c**, Phylogenetic analysis of repA-containing pAgos (orange

419 shaded) found from BLASTP against all isolates via JGI-IMG portal and other characterized pAgos. **d**, The

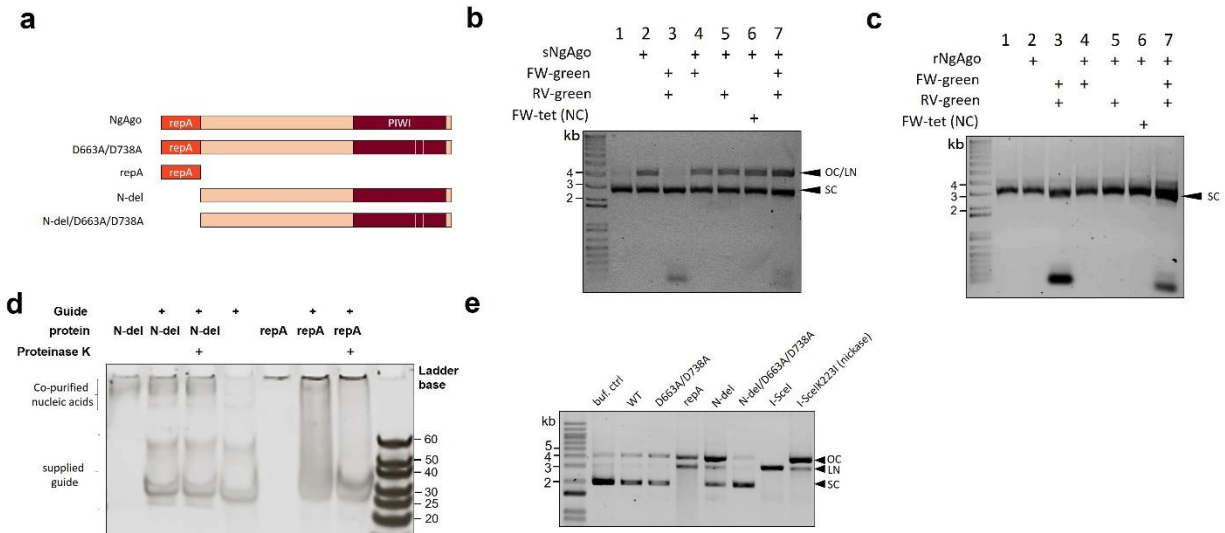
420 catalytic tetrad of NgAgo is conserved with catalytically active pAgos including MjAgo, PfAgo, MpAgo, and

421 TtAgo in sequence alignment. **e**, All residues of the catalytic tetrad (D663, E704, D738, and D863) DEDD,

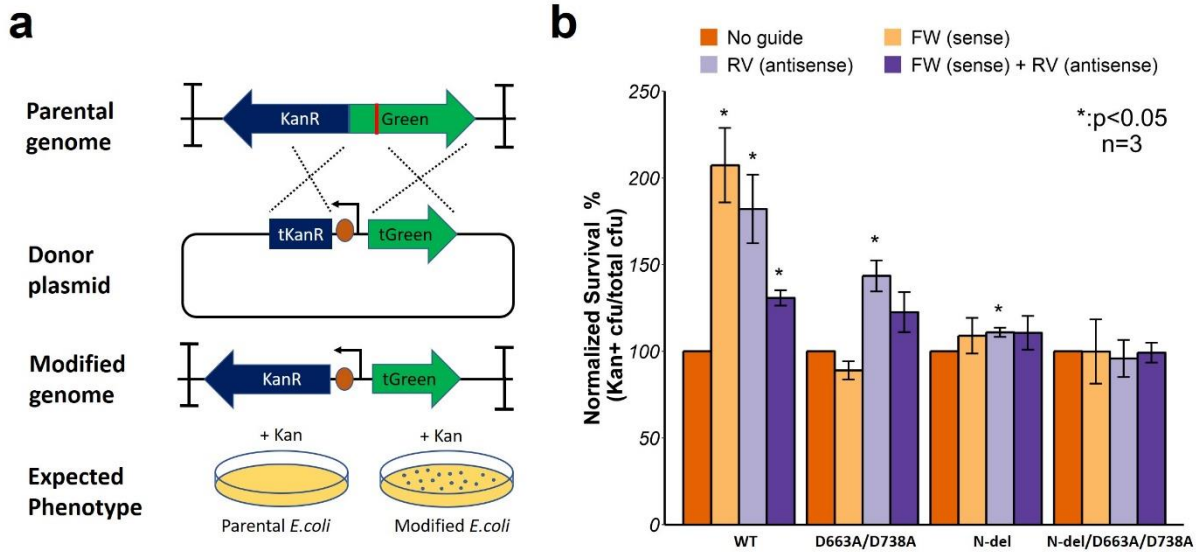
422 except E704 are structurally colocalized with the catalytic tetrad of MjAgo (D504, E541, D570, and D688).

423





424  
 425 **Figure 2 | Soluble NgAgo variants nick and cut plasmid DNA *in vitro* via repA and D663/D738**  
 426 **mutations in the PIWI domain. a**, NgAgo variants used in the *in vitro* assay to identify which domain is  
 427 essential for nicking and cleaving activity. **b**, Soluble NgAgo (sNgAgo) nicks and cuts plasmid DNA  
 428 regardless of the presence of guide DNA. **c**, Refolded NgAgo, rNgAgo, has no effect on plasmid DNA. **d**,  
 429 Electrophoretic mobility shift assay (EMSA) of N-del and repA domain with guides. N-del copurifies with  
 430 nucleic acids and does not bind (shift) supplied guide. repA does not copurify with nucleic acid and readily  
 431 binds and shifts supplied guide, confirming its single-stranded DNA binding ability. **e**, Plasmids were treated  
 432 with NgAgo variants for an hour before analysis on an agarose gel. Wildtype and D663A/D738A  
 433 incompletely nicks plasmids DNA while repA and N-del nick and cleave plasmids DNA. N-del/D663A/D738A  
 434 loses the ability to nick and cleave. I-SceI and I-SceI K223I are used as positive cleavage and nicking  
 435 controls, respectively. OC, open circular; LN, linear; SC, supercoiled.  
 436



437

438 **Figure 3 | NgAgo enhances gene-editing via  $\lambda$ -red-mediated homologous recombination in *E.coli*. a,**

439 Design of gene-editing assay in MG1655 (DE3). *KanR* and *mNeonGreen* (Green) cassette without promoter

440 and RBS, flanked by two double terminators, is integrated in MG1655 (DE3). Donor plasmid with truncated

441 *mNeonGreen* (tGreen) encodes a nonfunctional truncated *KanR* (tKanR). Guide was transformed to target

442 the *mNeonGreen* (red line). After successful gene editing, modified genome has a functional *KanR*

443 cassette, enabling survival in Kan selective plate. **b**, NgAgo variants enhance gene editing efficiency with

444 ~1 microgram of guide(s) relative to an unguided control. Error bars are the standard errors generated from

445 three replicates. Statistically significant results are indicated with \* ( $p$ -value < 0.05, paired t-test)

446

447

448 **Table 1. Strains and Plasmids**

Name	Relevant genotype	Vector backbone	Plasmid origin	Source
<b>Strains</b>				
BL21 (DE3)	F <sup>-</sup> ompT gal dcm lon hsdSB(rB <sup>-</sup> mB <sup>-</sup> ) λ (DE3) [lacI lacUV5-T7p07 ind1 sam7 nin5] [malB <sup>+</sup> ]K-12(λS)			29
MG1655 (DE3)	K-12 F <sup>-</sup> λ <sup>-</sup> ilvG <sup>-</sup> rfb-50 rph-1 (DE3)			30
MG1655 (DE3) <i>atpI</i> ::KanR-mNeonGreen	K-12 F <sup>-</sup> λ <sup>-</sup> ilvG <sup>-</sup> rfb-50 rph-1 (DE3) <i>atpI</i> ::KanR-mNeonGreen			This study
<b>Plasmids</b>				
pBSI-SceI(E/H)	<i>bla</i>		ColE1 derivative	31
pET32a-GST-ELP64	<i>bla</i> , lacI, P <sub>T7</sub> -GST-ELP64			Professor Xin Ge (University of California, Riverside)
pTKDP-hph	<i>bla</i> , <i>hph</i> , <i>sacB</i>		pMB1	32
pCas9-CR4	<i>cat</i> , P <sub>Tet</sub> -Cas9		p15A	33
pET-GST-Ago-His	<i>bla</i> , lacI, P <sub>T7</sub> -GST-NgAgo-His	pET32a-GST-ELP64	pBR322	This study
pET32a-His-Ago	<i>bla</i> , lacI, P <sub>T7</sub> -GST-NgAgo-His	pET32a-GST-ELP64	pBR322	This study
pET32a-His-repA	<i>bla</i> , lacI, P <sub>T7</sub> -His-repA	pET32a-GST-ELP64	pBR322	This study
pET-GST-N-del-His	<i>bla</i> , lacI, P <sub>T7</sub> -GST-N-del-His	pET32a-GST-ELP64	pBR322	This study
pET-GST-N-del/D663A/D738A-His	<i>bla</i> , lacI, P <sub>T7</sub> -GST-N-del/D663A/D738A-His	pET32a-GST-ELP64	pBR322	This study
pTKDP-KanR-mNeonGreen-hph	<i>bla</i> , <i>hph</i> , KanR-mNeonGreen	pTKDP-hph	pMB1	This study
p15-KanR-PtetRed	<i>cat</i> , KanR-mNeonGreen, P <sub>Tet</sub> -gam-beta-exo	pCas9-CR4	p15A	This study
pET32-BFP	<i>Amp</i> , lacI, P <sub>T7</sub> -BFP	pET32a-GST-ELP64 and pBAD-mTagBFP2	pBR322	This study